Journal of Coastal Research	00	0	000–000	Coconut Creek, Florida	Month 0000

Evaluation of Error Reduction Techniques on a LIDAR-Derived Salt Marsh Digital Elevation Model

Adam McClure[†]*, XiaoHang Liu[†], Ellen Hines[†], and Matthew C. Ferner[‡]

[†]Department of Geography and Environment
San Francisco State University
San Francisco, CA 94132, U.S.A.

[‡]San Francisco Bay National Estuarine Research Reserve
San Francisco State University
Tiburon, CA 94920, U.S.A.

www.cerf-jcr.org

www.JCRonline.org

ABSTRACT

McClure, A.; Liu, X.; Hines, E., and Ferner, M.C., 0000. Evaluation of error reduction techniques on a LIDAR-derived salt marsh digital elevation model. *Journal of Coastal Research,* 00(0), 000–000. Coconut Creek (Florida), ISSN 0749-0208.

Accurate elevation information is a necessity for conservation and management of tidal salt marshes where elevation differences can be as little as 2 m and where sea-level rise is a critical threat. We applied an existing method to evaluate and improve the vertical accuracy of a 1-m LIDAR-derived digital elevation model (DEM) using a real-time kinematic (RTK) GPS dataset with a vertical accuracy of ±0.02 m and local vegetation data within a tidal salt marsh. We generated correction factors for vegetation species within each major vegetation class and produced a modified DEM of the site. Comparison between the original and modified DEM showed that the mean error was reduced from 0.16 m to –0.004 m and the root mean squared error was reduced from 0.212 m to 0.098 m. These results demonstrate that it is possible to significantly reduce vertical error contained within a salt marsh DEM derived from a LIDAR dataset using highly accurate RTK GPS data combined with vegetation data collected on a per site basis.

ADDITIONAL INDEX WORDS: *DEM, China Camp State Park, National Estuarine Research Reserve, coastal vegetation, sea-level rise.*

INTRODUCTION

Tidal salt marshes and surrounding estuaries are among the world's most biologically productive ecosystems, providing commercial harvesting and recreational fishing opportunities that in California alone are estimated to produce statewide annual economic benefits between $6.3 billion and $22.9 billion (Allen *et al.*, 1992). These ecosystems provide detoxifying sites through chemical transformation of contaminants and aid in the stabilization of global nitrogen, atmospheric sulfur, carbon dioxide, and methane levels (Goals Project, 1999). Vegetation contained within tidal salt marshes in particular enhances water-purification processes and offers many species refuge from predators (Nicholls, Hoozemans, and Marchand, 1999; Reddy and Gale, 1994). Salt marshes protect inland areas against coastal flooding during storm-surge events, thereby decreasing risk to life and property (Arkema *et al.*, 2013; Nicholls, Hoozemans, and Marchand, 1999). They also shelter shorelines from waves and currents as sea-level rise (SLR) accelerates.

To preserve salt marshes, marsh elevation relative to the local tidal range must be monitored closely, as small deviations from established tidal marsh elevations can be critical to the ecology of a marsh. Studies have found that elevation differences of less than 10 cm can dictate species distributions (Silvestri, Defina, and Marani, 2005) and change salt marsh erosion and accretion rates (Vanderzee, 1988). If the relative tidal elevation of salt marshes declines, vegetated platforms will have the potential of converting to mudflats or open water, and both animal and plant species will undergo environmental stresses (Callaway, Nyman, and DeLaune, 1996). As global warming accelerates, SLR has become a major concern in regard to the preservation of tidal salt marshes. Understanding how tidal salt marshes respond to SLR and how SLR rates affect the temporal and spatial patterns of salt marsh accretion are thus becoming increasingly important (*e.g.*, Kirwan and Megonigal, 2013; Schile *et al.*, 2014; Stralberg *et al.*, 2011; Swanson *et al.*, 2013).

To accurately model various SLR scenarios and their consequences on these elevation- dependent ecosystems, a digital elevation model (DEM) possessing both high resolution and high accuracy is crucial (Gesch, 2009; Kirwan and Megonigal, 2013; Knowles, 2009; May, 2013). LIDAR is widely considered a promising technology in fulfilling such demand thanks to its unprecedented accuracy and resolution. LIDAR is an active remote sensing technology that emits laser beams to detect a surface. By measuring the time between transmission and reception, the distance between the sensor and the ground surface can be computed, thus enabling the inference of elevation and height information (El-Sheimy, Valeo, and Habib, 2005). Currently, the vertical error of LIDAR systems generally ranges from 0.10 m to 0.20 m (Hodgson and Bresnahan, 2004; Murakami *et al.*, 1999). LIDAR systems with a point density of 1 point/m^2 are commonly available (Ogilvie, 2014; USGS, 2013), and systems with 8–10 point/m^2 are becoming the norm with technology advancements (Heinzel and Koch, 2011; Hladik and Alber, 2012; Jakubowski, Guo, and Kelly, 2013). These characteristics of LIDAR make it the desired technology to acquire high-resolution elevation data in

DOI: 10.2112/JCOASTRES-D-14-00185.1 received 23 September 2014; accepted in revision 1 June 2015; corrected proofs received 28 August 2015; published pre-print online 24 September 2015.
*Corresponding author: adam.c.mcclure@gmail.com

areas with finely varying vertical relief (Rayburg, Thomas, and Neave, 2009; Webster and Dias, 2006), such as salt marshes.

Interestingly, the application of LIDAR in salt marshes has not been very successful. This is because the range of elevation in these vegetated habitats is usually less than 2 m, making small topographic differences very difficult to detect, even by LIDAR (Chassereau, Bell, and Torres, 2011; Hladik, Schalles, and Alber, 2013; Rosso, Ustin, and Hastings, 2006). In fact, it has been found that while the vertical error in LIDAR sensors is usually 0.10 m–0.20 m, the vertical error in LIDAR-derived DEMs within salt marsh sites can be up to 0.31 m (Hladik and Alber, 2012; Montane and Torres, 2006; Morris *et al.*, 2005; Sadro, Gastil-Buhl, and Melack, 2007; Schmid, Hadley, and Wijekoon, 2011). Such error far exceeds the accuracy requirements of short-term SLR impact analysis.

An alternative technology used to obtain more accurate elevation data is real-time kinematic (RTK) GPS, which is commonly used for surveying salt marshes. When using local bench marks, RTK GPS is capable of delivering horizontal and vertical accuracy as high as 0.01 to 0.02 m (Leica Geosystems, 2013), which is nearly 10 times as accurate as current LIDAR systems. However, it is impossible to acquire RTK GPS points in salt marshes at a density similar to that of LIDAR. This is because while LIDAR acquires elevations remotely, RTK GPS has to collect elevations in the field. Costs to survey a large area can be prohibitive, not to mention the difficult ground access and ecological sensitivity (Athearn *et al.*, 2010). Considering that DEM accuracy is highly correlated with sample density (Hu, Liu, and Hu, 2009; Wilson, 2012), RTK GPS points alone will not provide adequate data to create a high-accuracy DEM (Liu *et al.*, 2012). It is possible, however, to use RTK GPS data to calibrate and supplement LIDAR-acquired elevations during DEM generation so that errors in LIDAR-derived DEMs may be effectively reduced (Hladik and Alber, 2012; Sadro, Gastil-Buhl, and Melack, 2007).

In addition to RTK GPS data, local vegetation data have also been found to benefit topographical modeling. One problem with using LIDAR in vegetated areas is that LIDAR-laser returns often cannot fully penetrate dense vegetation, thus leading to a misrepresentation of the ground surface (Rosso, Ustin, and Hastings, 2006; Schmid, Hadley, and Wijekoon, 2011; Webster and Dias, 2006). This also applies to salt marshes, as noted by Montane and Torres (2006) and Chassereau, Bell, and Torres (2011) from their research at a reserve in South Carolina. If local vegetation data are available, however, vegetation-specific correction factors may be generated to calibrate a LIDAR-derived DEM. Research by Hladik and Alber (2012) in a salt marsh in Georgia showed that this method can significantly reduce the overall mean error (ME) from 0.10 m to –0.01 m. The same method was used again the following year as part of a study that used hyperspectral data to modify a LIDAR-derived DEM, which achieved similar results (Hladik, Schalles, and Alber, 2013).

In this research, we examine the effectiveness of using both RTK GPS and vegetation data to reduce the errors in a LIDAR-derived DEM of a salt marsh on the Pacific coast. While similar error production techniques have been applied before, all previous studies were conducted along the Atlantic coast. Tidal marsh environments in these areas are expansive and consist of broad coastal floodplains (Phinn, Stow, and Zedler, 1996; Zedler, 1991). Salt marsh vegetation is relatively homogeneous along these coastlines and is often dominated by a single species, *Spartina alterniflora* (Zedler *et al.*, 1999), though other species also exist (Hladik and Alber, 2012; Hladik, Schalles, and Alber, 2013; Schmid, Hadley, and Wijekoon, 2011). In comparison, Pacific coast salt marshes such as those in the San Francisco Bay (SF Bay) are typically smaller in size, fragmented with complex creek networks, and characterized by high vegetation diversity; descriptors that make evaluating these environments using remote sensing techniques more difficult (Byrd *et al.*, 2014; Byrd, Kelly, and Dyke, 2004; Zedler *et al.*, 1999). Whether RTK GPS and vegetation data can effectively reduce vertical error contained within a LIDAR-derived DEM in these areas is still unknown. In the literature, Sadro, Gastil-Buhl, and Melack (2007) used vegetation data to improve a LIDAR salt marsh DEM in southern California. Their accuracy assessment was only carried out on the unmodified DEM, however. Within SF Bay, Rosso, Ustin, and Hastings (2006), Schile *et al.* (2014), and Stralberg *et al.* (2011) have applied techniques to reduce error in LIDAR salt marsh DEMs, but these studies have lacked either vegetation-specific corrections or a detailed vertical accuracy assessment. In contrast, our research provides the first comprehensive analysis on the effectiveness of using RTK GPS and vegetation data to reduce vertical error in a LIDAR-derived DEM on a Pacific coast salt marsh. Findings and lessons from this case study will inform future studies along the Pacific coast where a detailed understanding of marsh responses to SLR is needed to help prioritize conservation and restoration opportunities.

METHODS

Our study site was a salt marsh in China Camp State Park, hereafter referred to as China Camp. Located approximately 25 km north of the city of San Francisco, China Camp borders the SW edge of San Pablo Bay in Marin County, California (Figure 1). Vegetation within the site primarily consists of five species (Figure 2). *Salicornia pacifica* covers the largest area of marsh surface and dominates the relatively high salt marsh platform. Known as a preferred habitat for the *Rallus longirostris obsoletus*, *S. pacifica* is interspersed with tidal creeks, and its canopy height is typically between 0.2 m and 0.4 m (Baye, 2012; Wood *et al.*, 2012). Another vegetation species is *Spartina foliosa*, which is found along the low fringing tidal marsh, a transitional area between salt marsh and mud flats, and can grow up to heights of 1.2 m (Nordby, Cohen, and Beissinger, 2009). Three other less dominant vegetation species cover a variety of locations. *Bolboschoenus maritimus* is found sporadically populating low marsh areas between *S. pacifica* and *S. foliosa* and has a height range of 0.08–1.5 m (Kantrud, 1996). *Grindelia stricta*, with a canopy height of up to 1 m (Nordby, Cohen, and Beissinger, 2009), is known as an important habitat for the state endangered *Laterallus jamaicensis coturniculus* (California National Diversity Database, 2013) and is found primarily on natural berms alongside tidal creeks (Baye, 2012; Wood *et al.*, 2012). *Distichlis spicata* has a height range of 0.15–0.45 m at maturity (Hauser, 2006) and is located throughout the tidal marsh platform area and along the terrestrial-marsh ecotone.

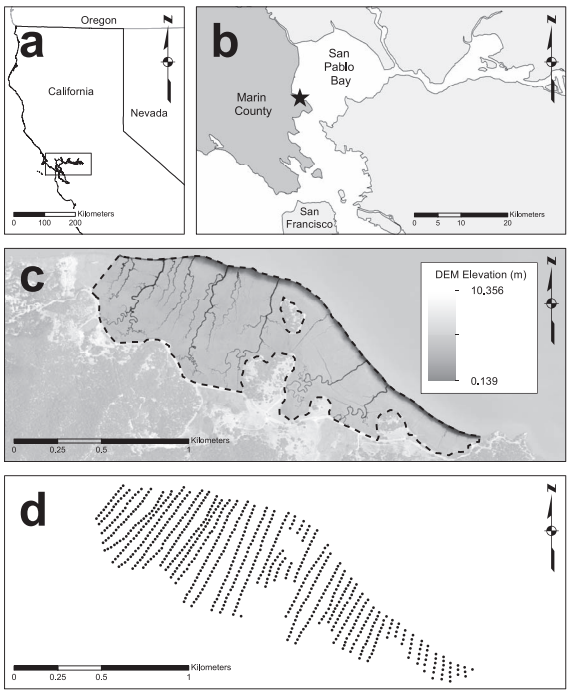

Figure 1. (a) Study site location along the west coast of California. (b) Study site location within San Francisco Bay. (c) USDA National Agriculture Imagery Program (USDA, 2009) aerial image with original LIDAR-derived DEM overlay (Hines, 2011). (d) RTK GPS survey point locations within study site boundary (USGS, 2013).

Golden Gate LIDAR Project LIDAR Survey

We used LIDAR data from the Golden Gate LIDAR Project (GGLP), which collected data for the United States Geological Survey (USGS) National Map (USGS, 2015) for Marin and San Francisco Counties along with portions of San Mateo and Sonoma Counties between the months of April and July of 2010 during the lowest tides possible (Hines, 2011). All horizontal data were projected in North American Datum of 1983 (National Oceanic and Atmospheric Administration [NOAA] National Geodetic Survey [NGS]), and their accuracy was less than 1 m based on a minimum point density of 2 points/m^2. Vertical data were collected in North American Vertical Datum of 1988 (NOAA NGS) and have an accuracy of less than or equal to 0.0925 m when measured as root mean squared error (RMSE) (Hines, 2011). Further detail regarding LIDAR acquisition for the dataset used in this study is provided in Table 1.

Over 18 million points were extracted from the GGLP dataset for this study. These LIDAR points were filtered with TerraScan to produce a set of points classified as bare-earth ground (Hines, 2011). This filtered set of points was then cropped based on the study site boundary. A triangulated irregular network (TIN) was built based upon the bare-earth LIDAR points within the study site. The TIN was then converted to a 1-m resolution DEM using the TIN-to-Raster tool in ArcGIS software (ESRI, 2013). Details of the TIN-to-Raster conversion can be found in Hu, Liu, and Hu (2009). This DEM is hereafter referred to as the Original DEM.

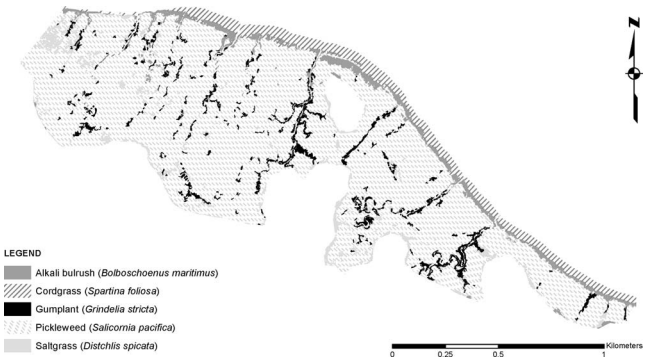

Figure 2. Vegetation distribution within the study site based on a color infrared image classified using the maximum likelihood method (NOAA, OCM, 2012).

RTK GPS Survey

A set of 753 RTK GPS points were collected over 0.967 square km of salt marsh (Figure 1d) located along the NE edge of China Camp between February and March 2010 by the USGS Western Ecological Research Center as part of a comprehensive study of SLR modeling of 12 salt marshes within SF Bay (Takekawa *et al*., 2013). Elevation points were recorded with a Leica RX1200 RTK GPS rover with a horizontal accuracy of ±1 cm and a vertical accuracy of ±2 cm (Leica Geosystems, 2013). The WGS84 ellipsoid model was used for both horizontal and vertical positioning, measuring vertical error within 2.5 cm throughout the study. An elevation point was measured every 25 m along transect lines separated by 50 m with no points collected within tidal creeks (Takekawa *et al*., 2013).

Vegetation Classification Map

A vegetation classification map of China Camp, which has served as the baseline habitat map for the San Francisco Bay National Estuarine Research Reserve China Camp Component, was obtained from NOAA. This map has been used to identify marsh areas likely to be most susceptible to changes in inundation and to prioritize areas for monitoring and restoration planning. The map was created based on a 0.25-m resolution color-infrared (CIR) aerial image acquired on 26 July 2006 (NOAA, OCM, 2012). This CIR image was classified using a training set of 31 GPS points, which were collected in November 2005, to represent the dominant vegetation species. The classification method used was the maximum likelihood algorithm in the ArcGIS Multivariate Toolbox. The classification result was assessed using 176 points randomly generated by NOAA personnel within the study site in February 2008. Each of the 176 points was located in the field using a GPS receiver; the dominant species within a 1-m radius was recorded for each point. These 176 GPS points are separate from the 753 RTK GPS data points introduced previously in the "RTK GPS Survey" section. The overall accuracy of the classification was 91%, and the Kappa statistics were 82% for six vegetation species, five of which are found within our study

Table 1. *LIDAR flight and sensor system specifications during acquisition for the Golden Gate LIDAR Project (GGLP) dataset.*

Sensor	Leica ALS60 MPiA
Aircraft	Cessna 207
Flight Date	April, July 2010
Altitude (m above ground level, nominal)	2000
Swath Width (m, nominal)	1454
Sidelap (%, minimum)	20
Number of Spectral Bands	1
Wavelengths (nm, coherent pulsed laser source)	1064
Field of View (°, nominal)	40 (±20 from nadir)
Laser Pulse Repetition Frequency (kHz, nominal)	120
Scan Frequency (Hz, nominal)	85
Scan Angle (°, nominal)	40
Nominal Post Spacing (pts/m^2)	2 minimum

area (Figure 2). These five vegetation species are *B. maritimus, S. foliosa*, *G. stricta*, *S. pacifica*, and *D. spicata*. Table 2 summarizes the areal coverage of these vegetation species, their elevations in the Original DEM, and their classification accuracy in terms of user's accuracy. It can be seen that although all other vegetation species were classified fairly accurately, the accuracy of *B. maritimus*, which has the least areal coverage, was only 33%.

Accuracy Assessment of Original DEM

Using a similar method to Hladik and Alber (2012) and Hladik, Schalles, and Alber (2013), we assessed DEM vertical accuracy by overlaying RTK GPS points on the Original DEM. RTK GPS elevation values were assumed to be the true ground elevation. The elevation of the cells containing RTK GPS points was extracted from the Original LIDAR-derived DEM and compared to the RTK GPS elevation. A comparison of the overall site was conducted first, followed by assessments in each of the five vegetation species listed in Table 2.

For each vegetation-specific accuracy assessment, the error at point i, denoted as Δz_i, was calculated by $\Delta z_i = z_{\mathrm{LIDAR}_i} - z_{\mathrm{RTK}_i}$, where z_{RTK_i} was the elevation of the ith RTK GPS point and z_{LIDAR_i} was the elevation of the cell in the Original DEM, which contained the RTK GPS point. The errors were then summarized using the following statistics: ME, standard deviation (SD), RMSE, fundamental vertical accuracy (FVA), and 95th percentile. ME is the mean of all errors, *i.e.* $\mathrm{ME} = (\sum \Delta z_i)/n$. RMSE, which is routinely used in DEM accuracy assessments, is calculated using the following formula:

$$\mathrm{RMSE} = \sqrt{\frac{\sum(\Delta z_i)^2}{n}} = \sqrt{\frac{\sum(z_{\mathrm{LIDAR}_i} - z_{\mathrm{RTK}_i})^2}{n}}$$

RMSE can be interpreted as SD if the errors are normally distributed and contain random errors only (NDEP, 2004). Otherwise, RMSE is best interpreted as the average magnitude of the errors (Liu *et al.*, 2012). FVA, also known as the 95% confidence interval, is calculated as $1.96 \times \mathrm{RMSE}$. This statistic is useful when DEM errors have a normal distribution (Flood, 2004). In the case of nonnormal distribution, the 95th percentile, which means 95% of errors are less than or equal to this value, should be used (Flood, 2004; NDEP, 2004). To determine whether the vertical errors follow a normal distribution, we calculated the skewness of the errors in the Original DEM and Modified DEMs, first using all errors in each DEM and then using the errors in each vegetation species. A skewness value beyond the range of [–0.5, 0.5] suggests nonnormal distribution (Flood, 2004).

DEM Modification Using RTK GPS and Vegetation Data

A correction factor was generated for each vegetation species by calculating the corresponding ME. ME of the overall study site was calculated as well to be later used to modify areas devoid of vegetation. When generating each correction factor, 75% of the RTK GPS points bound by that vegetation class (or the entire study site for the site-wide correction factor) were randomly selected to serve as training points. The remaining 25% of the RTK GPS points served as test points. Elevations of the training points in the Original DEM were extracted and compared with the elevation values provided by RTK GPS. The ME of these training points was calculated and used as the correction factor to modify the elevations in that vegetation class. Accuracy of the modified elevations was assessed using the 25% test points and reported in ME, SD, RMSE, FVA, and 95th percentile. Because of a relatively small number of RTK GPS points for *B. maritimus, S. foliosa, G. stricta*, and *D. spicata*, bootstrapping was used when evaluating these species to obtain reliable statistics. Specifically, the 75%–25% partition process described previously was repeated 30 times for each of the four species. During each iteration, ME, SD, RMSE, FVA, and 95th percentile were calculated using test points. The average of the 30 iterations was used to describe the accuracy of the modified elevations in *B. maritimus*, *S. foliosa*, *G. stricta*, and *D. spicata*.

Table 2. *Summary of vegetation height, areal coverage, elevation statistics, and classification accuracy for each vegetation type and the entire study site. All elevation statistics were calculated based on the Original 1-m LIDAR-derived DEM and describe minimum, maximum, mean, and standard deviation (SD) values in m. Areal coverage was based on the vegetation map created by classifying a color infrared imagery using the maximum likelihood method. Classification accuracy values are the user's accuracy for each vegetation species, as well as the overall accuracy for the entire site (NOAA, OCM, 2012).*

Vegetation Class	Height (m)	km^2	% cover	Elevation Statistics (m)				Classification Accuracy (%)
				Min	Max	Mean	SD	
Bolboschoenus maritimus	0.08–1.5	0.031	3.2	0.262	7.554	1.845	0.329	33
Spartina foliosa	≤1.20	0.065	6.7	0.139	2.274	1.172	0.325	100
Grindelia stricta	≤1.00	0.033	3.4	0.221	2.496	1.764	0.405	83
Salicornia pacifica	0.20–0.40	0.765	79.1	0.152	6.135	1.963	0.167	93
Distichlis spicata	0.15–0.45	0.032	3.3	0.384	5.489	1.969	0.278	100
No vegetation	-	0.041	4.3	-	-	-	-	-
Overall	-	0.967	100.0	0.139	10.356	1.886	0.348	92

Table 3. *Accuracy assessment of the Original DEM with* n *indicating the number of samples used to calculate mean error (ME), standard deviation (SD), root mean squared error (RMSE), fundamental vertical accuracy (FVA), and 95th percentile. ME values were used as species-specific correction factors to create the Modified DEM. Except* S. pacifica *and overall classes, all values were obtained using boostrapping. All values are in m.*

Vegetation Class	*n*	ME	SD	RMSE	FVA	95th Percentile
Bolboschoenus maritimus	14	0.255	0.176	0.310	0.608	0.437
Spartina foliosa	12	0.215	0.073	0.226	0.443	0.314
Grindelia stricta	16	0.103	0.202	0.215	0.421	0.260
Salicornia pacifica	480	0.170	0.104	0.199	0.390	0.292
Distichlis spicata	19	0.148	0.109	0.184	0.361	0.258
Overall	564	0.160	0.139	0.212	0.416	0.301

The ME value of each vegetation class was used as the correction factor for that species throughout the site. The Modified DEM was obtained by subtracting the vegetation-specific correction factors from the Original DEM. Areas devoid of vegetation were modified using the site-wide correction factor. The accuracy of the Modified DEM was assessed using the 25% RTK GPS points saved as test points for the overall study site.

RESULTS

Overall, the Original DEM had a ME of 0.160 m and a RMSE of 0.212 m, and 95% of the vertical errors were equal to or less than 0.301 m (Table 3). Among vegetation species, *B. maritimus* produced the largest ME, RMSE, and 95th percentile values. *G. stricta* produced the smallest ME, and *D. spicata* produced the smallest RMSE and 95th percentile. Unlike other vegetation classes whose vertical errors in the Original DEM have both overestimations and underestimations, ground elevations in the *S. foliosa* class were consistently overpredicted in the Original DEM. In terms of correction factors, which are the ME values in Table 3, the largest correction factor of 0.255 m was for *B. maritimus*, and the smallest correction factor of 0.103 m was for *G. strica*. The correction factor of 0.170 m was applied to the largest amount of the marsh surface because of the dominance of *S. pacifica*.

After the correction factors (ME) in Table 3 were applied, an accuracy assessment was conducted on the Modified DEM. The overall ME was reduced to –0.004 m, RMSE was reduced to 0.098 m, and 95% of the vertical errors were equal to or less than 0.137 m (Table 4). *B. maritimus* still had the largest ME (–0.018 m) among all classes; however, the sign of its ME changed during DEM modification, suggesting that while overestimation errors were effectively reduced, underestimation errors were worsened in some areas. Large RMSE values were still associated with tall vegetation species such as *B. maritimus* (0.202 m) and *G. stricta* (0.200 m), and short vegetation species such as *S. pacifica* (0.106 m) and *D. spicata* (0.087 m) continued to have smaller RMSEs. The RMSE of *S. foliosa*, which is similar to *B. maritimus* and *G. stricta* in height but had much higher classification accuracy in the vegetation map, was reduced to 0.073 m. Regardless of their RMSE values, the 95th percentile of all vegetation species were less than or equal to 0.142 m, and the overall 95th percentile was 0.137 m. This suggests that even in *B. maritimus* and *G. stricta* habitats, which had the largest RMSEs after modification, only 5% of their errors were more than 0.142 m. Interestingly, the largest 95th percentile was found in *S. pacifica* (0.142 m), whose RMSE (0.106 m) was much smaller compared to *B. maritimus* (0.202 m). This is most likely because *B. maritimus* had more negative errors than *S. pacifica*, which also explained why the ME of *B. maritimus* (–0.018 m) was negative while the ME of *S. pacifica* (0.002 m) was positive.

DISCUSSION

As shown in Figure 3, there are both overestimation and underestimation errors in the Original and Modified DEMs, although the majority of errors in both DEMs were attributable to overestimation. Overestimation of a LIDAR-derived DEM ground surface within a salt marsh has been noted in previous studies on both Atlantic and Pacific coasts (Hladik and Alber, 2012; Montane and Torres, 2006; Morris *et al*., 2005; Sadro, Gastil-Buhl, and Melack, 2007; Schmid, Hadley, and Wijekoon, 2011). In our study, 95% of the ground elevations were overestimated. A skewness test based on the errors in the Original and Modified DEM, respectively, suggest that the errors in neither DEM follow a normal distribution (Figure 3). Nonnormal distribution was also observed when testing skewness for individual vegetation species. These results suggest that FVA values, which are based on the assumption of normal distribution, are not useful in this research. Instead, 95th percentile vales should be used.

Multiple sources contributed to the error in the Original DEM. According to the accuracy assessment framework by Liu *et al*. (2012), error in a DEM is the sum of two components:

Table 4. *Accuracy assessment of the Modified DEM with* n *indicating the number of samples used to calculate mean error (ME), standard deviation (SD), root mean squared error (RMSE), fundamental vertical accuracy (FVA), and 95th percentile. Except* S. pacifica *and overall classes, all values were obtained using bootstrapping. All values are in m.*

Vegetation Class	*n*	ME	SD	RMSE	FVA	95th Percentile
Bolboschoenus maritimus	9	−0.018	0.181	0.202	0.395	0.136
Spartina foliosa	4	0.002	0.067	0.073	0.142	0.068
Grindelia stricta	6	0.004	0.189	0.200	0.391	0.140
Salicornia pacifica	159	0.002	0.106	0.106	0.207	0.142
Distichlis spicata	6	0.011	0.087	0.087	0.170	0.102
Overall	189	−0.004	0.098	0.098	0.191	0.137

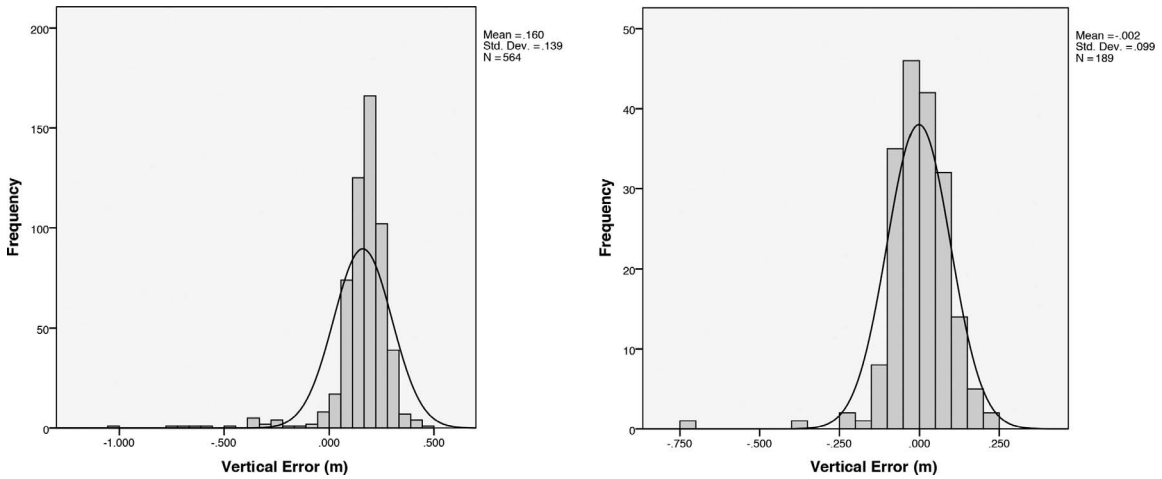

Figure 3. (a) Histogram of vertical errors within the original DEM using 75% of the RTK GPS points. (b) Histogram of vertical errors within the modified DEM using 25% of the RTK GPS points.

error in the source data and error introduced by interpolation. Previous research has derived that the error introduced by interpolation is determined by curvature and point density (Hu, Liu, and Hu, 2009). Given that tidal salt marshes are relatively flat, interpolation error can be expected to be negligible. Thus, error in the Original DEM was mainly attributable to the error in the source data, which are the bare-earth LIDAR points used to derive the DEM. Such an error includes both the error in the LIDAR system and the error caused by the laser's difficulty to penetrate the salt marsh vegetation canopy, a problem similarly noted in previous LIDAR studies (Hladik and Alber, 2012; Morris *et al*., 2005; Rosso, Ustin, and Hastings, 2006; Sadro, Gastil-Buhl, and Melack, 2007; Schmid, Hadley, and Wijekoon, 2011). Because the RMSE of the Original DEM was 0.212 m and the RMSE of the LIDAR system was 0.0925 m, we estimate the RMSE of the error attributable to other factors such as canopy penetration difficulty and vegetation classification error to be approximately 0.120 m. Although we realize that RMSE is a descriptor of DEM errors on a flat, paved surface and that we are calculating RMSE on a vegetated surface, RMSE is still widely used as a descriptor of error within a DEM. Methods and standards are currently under review that would allow for future DEM accuracy assessments on vegetated terrain (Coleman, 2014).

The error in the Original DEM varied from species to species. Larger RMSEs were found in tall species such as *B. maritimus* (0.310 m), *S. foliosa* (0.226 m), and *G. stricta* (0.215 m), while smaller RMSEs were found in short species such as *S. pacifica* (0.199 m) and *D. spicata* (0.184 m). One explanation is that taller vegetation species can form a canopy that is difficult for LIDAR to penetrate. In the case of *B. maritimus*, its height can range from 0.08 m to 1.5 m (Kantrud, 1996), and its maximum height is greater than any other species within the study site. Similarly, *S. foliosa* and *G. stricta* both have a height of more than 1.0 m, which is much taller than the height of *S. pacifica* and *D. spicata*, which ranges from 0.20 to 0.40 m and 0.15 to 0.45 m, respectively. Yet, height is not the only factor affecting LIDAR laser penetration (Sadro, Gastil-Buhl, and Melack, 2007). Stem density, biomass, and leaf orientation can also prohibit LIDAR sensors from fully reaching bare earth at marsh locations (Hodgson and Bresnahan, 2004; Rosso, Ustin, and Hastings, 2006; Schmid, Hadley, and Wijekoon, 2011). In our study, the LIDAR data were acquired between April and July, the primary growing season for salt marsh vegetation. *B. maritimus* can produce flowerhead clusters with three long leaf bracts (Baye, 2007) and can form dense colonies, another factor that could have contributed to canopy penetration difficulty. In comparison, *S. pacifica* is erect, shrubby, and highly branched (Baye, 2012), which could have allowed a greater chance for laser penetration.

Another source of error in the Original DEM is vegetation classification accuracy. In our study, *B. maritimus* has the poorest classification accuracy (33%) followed by *G. stricta* (83%). *B. maritimus* and *G. stricta* are both the least dominant species in our study site, each occupying only 3.2% to 3.4% of the total area. The habitat of *B. maritimus* is also adjacent to the habitat of *S. foliosa*, two species that have been known to be difficult to differentiate when using remote sensing techniques during drought years (Baye, 2012). Furthermore, both *B. maritimus* and *S. foliosa* are located downslope from the rest of the salt marsh and can become smothered by dense *S. pacifica* litter (Baye, 2012), allowing an opportunity for further laser obstruction and classification confusion. *G. stricta* is bushy and highly branched, and its distribution follows tidal creek edges (Figure 2). In contrast, *S. pacifica* and *D. spicata* both possessed very high classification accuracy, 93% and 100%, respectively. *S. pacifica* dominated nearly 80% of the study site, and *D. spicata* is dominantly found in sloping areas of the terrestrial-marsh ecotone. These reasons explain why *S. pacifica* and *D. spicata* contained smaller errors than that of *B. maritimus*, *S. foliosa*, and *G. stricta*.

Error in the Original DEM was reduced significantly after applying vegetation-specific correction factors. The RMSE of the Modified DEM was 0.098 m, and 95% of the errors were less

than or equal to 0.135 m (Table 4). A closer look at each vegetation class revealed that the RMSE of *S. foliosa* (0.073 m), *D. spicata* (0.087 m), and *S. pacifica* (0.106 m) species are close to the RMSE of the LIDAR sensor (0.0925 m), indicating that most nonsensor errors such as those attributable to laser penetration difficulty have been removed. *B. maritimus* saw a nearly 50% reduction in RMSE, but its RMSE (0.202 m) is still the largest among all species. The RMSE of *G. stricta* (0.200 m) remained nearly the same after modification. However, its 95th percentile was reduced from 0.260 m to 0.140 m, signifying that many overestimation errors in *G. stricta* in the Original DEM have been corrected.

The maximum vegetation-specific correction factor (ME) in our study was 0.255 m (*B. maritimus*), which was identical to that found by Hladik and Alber (2012). However, the minimum correction factor in our study was 0.103 m (*G. strica*), which was 0.06 m greater than that found by Hladik and Alber (2012). When compared to Sadro, Gastil-Buhl, and Melack (2007), the only other study that produced vegetation-specific correction factors for a salt marsh DEM on the Pacific coast, our maximum vegetation-specific correction factor was 0.07 m greater, and our minimum correction factor was 0.03 m less. These results suggest that vegetation-specific correction factors vary from location to location, depending on vegetation type and the data used during modification. For Rosso, Ustin, and Hastings (2006), who found the heights of live and dead canopies of *S. foliosa* and *S. pacifica* at a site located south of China Camp ranging from 0.15 m to 0.80 m, their vegetation-specific correction factor would likely be different from ours, even though their study site was located in SF Bay. Similarly, because Wang *et al*. (2009) found that using their 8 points/m^2 LIDAR over a salt march in Italy resulted in an underestimation of the vegetation canopy top by 0.177 m, their correction factor would most likely be around 0.177 m, a smaller value than the 0.255 m found in our research. Schmid, Hadley, and Wijekoon (2011) reported a ME of 0.150 m for *S. alterniflora* in a marsh area in South Carolina. Had they created a correction factor for this species, the value would likely be 0.150 m instead of the 0.03 m–0.27 m, as in Hladik and Alber (2012). These studies suggest that vegetation-specific correction factors are location and data dependent. They must be generated according to vegetation type and salt marsh location using the LIDAR and GPS data available.

To evaluate the effectiveness of our error reduction, we compared the accuracy of our Original and Modified DEMs with those found in Hladik and Alber (2012). For the errors in the Original DEM, the overall ME was 0.160 m in our research and 0.10 m in Hladik and Alber (2012). Similarly, overall RMSE was 0.212 m in our research and 0.16 m in Hladik and Alber (2012). These values suggest that our Original DEM contained more errors than the Original DEM in Hladik and Alber (2012). This was confirmed when comparing the vegetation-specific statistics between the two studies. Because of the difference in vegetation species, a direct comparison was not informative. Vegetation-specific MEs in our study ranged from 0.103 m to 0.255 m, whereas those found in Hladik and Alber (2012) ranged from 0.01 m to 0.27 m. RMSEs in Hladik and Alber (2012) ranged from 0.04 m to 0.31 m with all vegetation species except tall *S. alterniflora* being less than 0.18 m. In contrast, all of the vegetation species in our study had a RMSE of more than 0.18 m, with the largest RMSE being also 0.31 m. Comparisons using the 95th percentile in both studies further confirmed that the Original DEM in our study contained more errors than the counterpart in Hladik and Alber (2012).

Despite the significant differences between the Original DEMs in these two studies, the Modified DEM in our study matched more closely with that found in Hladik and Alber (2012). After applying vegetation-specific correction factors, the overall ME in our Modified DEM became –0.004 m compared to –0.01 m in Hladik and Alber (2012). Overall RMSE in our Modified DEM was 0.098 m, whereas the RMSE in Hladik and Alber (2012) was 0.10 m, and 95% of the vertical errors in our Modified DEM were 0.137 m or lower, whereas 95% of the vertical errors in the Modified DEM in Hladik and Alber (2012) were 0.17 m or lower. These statistics suggest that our Modified DEM was more accurate than the Modified DEM produced by Hladik and Alber (2012). In both studies, the largest RMSE value of 0.31 m, which was found in tall *S. alterniflora* in Hladik and Alber (2012) and *B. maritimus* in our study, was reduced by nearly 50%. On the other hand, our vegetation-specific RMSEs and 95th percentiles remained higher than those in Hladik and Alber (2012) even after modification. This can be most likely attributed to the different methods used to produce vegetation maps and the difference in salt marsh vegetation composition and density between the Pacific coast and the Atlantic coast. In addition, Hladik and Alber (2012) used four test sites within their study site to generate vertical accuracy statistics. In comparison, we generated statistics based on the entire study site. Side-by-side comparisons between the Original and Modified DEMs produced during this study suggest that the error reduction method based on using vegetation-specific correction factors can be applied to salt marshes in the Pacific Coast as effectively as, if not more so than, salt marshes located along the Atlantic Coast.

Although our results highlight significant vertical error reduction within the Original LIDAR-derived DEM, the Modified DEM is still not adequate for some salt marsh applications. For example, to model the impact of SLR, NOAA's rule of thumb is that the vertical error of a DEM should be at least twice as certain as the SLR increment (NOAA, 2010). The California Climate Action Team (2013) estimates that SLR for coastal areas south of Cape Mendocino, which includes our study site, is projected to be 0.15 m between the years of 2000 and 2030, 0.305 m between 2000 and 2050, and 0.835 m between 2000 and 2100. Given these SLR increments, the corresponding DEM must have a vertical accuracy of 0.075 m, 0.153 m, and 0.418 m, respectively, to reliably map SLR vulnerability. The Modified DEM in this research has a RMSE of 0.098 m, meaning it is suitable for modeling SLR impact between 2000 and 2050 or between 2000 and 2100, but not between 2000 and 2030. In fact, given that the LIDAR system used in this research has an RMSE equal to or less than 0.0925 m, even if there was no additional error introduced by laser penetration or vegetation classification, the LIDAR elevation data would still not be accurate enough for near-term SLR impact analysis between 2000 and 2030. More advanced

LIDAR technology possessing lower sensor error and higher penetration ability is necessary. While full-waveform LIDAR allows for digitization and a full recording of the complete backscatter signal, software and technical limitations presently exclude this type of LIDAR from common commercial usage. This being said, others have suggested that full-waveform LIDAR can be used to deliver improved elevation data in marsh and coastal areas with the ability to detect different types of vegetation (Schmid, Hadley, and Wijekoon, 2011; Wagner *et al*., 2004).

In addition to using advanced LIDAR technology, further improvement on the Original DEM can be obtained by increasing the number of RTK GPS points. In our study, all vegetation species except *S. pacifica* had a limited number of training and test points. Although we used bootstrapping to assure statistical validity, an increased number of RTK GPS points would help generate more accurate and robust correction factors. The American Society of Photogrammetry and Remote Sensing guideline requires 30 samples per vegetation species (Flood, 2004) based on the assumption that DEM errors are normally distributed. Because both overall and vegetation-specific DEM errors in this study were found not to be normally distributed, more than 30 samples are necessary for each vegetation species. On the other hand, the sensitivity of salt marsh ecosystems and the cost of field data collection dictate that proper planning and extreme care must be practiced so that the salt marsh is exposed to the least amount of physical harm during RTK GPS surveying. Considering that this study site is home to federally endangered endemic species such as *Reithrodontomys raviventris* and *R. longirostris obsoletus*, as well as the previously mentioned state of California threatened *L. jamaicensis coturniculus* (California National Diversity Database, 2013), a useful direction of future research would be to assess the minimum amount of additional RTK GPS points needed for each vegetation species and their distribution. Additionally, we recommend collecting vegetation height and species data for all points when collecting RTK GPS points, thereby allowing for the production of height groups within vegetation classes, which could be used to further refine correction factors.

Another strategy for further improvement is site-specific vegetation mapping. Hyperspectral and aerial images are often collected concurrently with LIDAR data and have been used in previous salt marsh DEM research (Hladik, Schalles, and Alber, 2013). Images taken concurrently provide the opportunity to obtain a highly accurate vegetation classification. In the case that concurrent images are not available, care should be exercised to minimize the temporal gap between LIDAR data and vegetation mapping. In our research, the temporal gap between the aerial imagery used to classify vegetation and LIDAR datasets was larger than desired; however, the vegetation map we used was the only one available for the study site at this time. Additionally, planning a future LIDAR flight during times when the marsh has the least biomass accumulated (*i.e*. leaf-off conditions during a dry season) could reduce vertical error because of laser penetration.

The error reduction technique used in this study as well as in previous salt marsh studies (Hladik and Alber, 2012; Hladik, Schalles, and Alber, 2013; Sadro, Gastil-Buhl, and Melack, 2007; Schile *et al*., 2014) addressed only the vertical accuracy aspect of a LIDAR-derived DEM. Other accuracy aspects of a DEM, such as its ability to preserve sequence and terrain structure (*e.g*., peaks, pits, ridges, valleys, passes), are also important but are beyond the scope of this study. For the purpose of salt marsh preservation, different applications have different accuracy requirements. For example, SLR vulnerability analysis affects mostly the vertical accuracy of a DEM because the result depends directly on absolute elevation values; however, for other salt marsh analysis such as topographical feature analysis in tidal creeks and coastal environment monitoring, the ability of a DEM to preserve elevation sequence signifies far more than a DEM's vertical accuracy. A DEM may produce fairly accurate estimates of the elevation at two points a and b; however, if this DEM suggests a is higher than b while the truth is the opposite, then this DEM will not be useful to derive topographical features or flow directions despite its high vertical accuracy (Liu, Hu, and Hu, 2014). The way to create DEMs that preserve elevation sequence and terrain skeleton is still under investigation (Liu, Hu, and Hu, 2014).

CONCLUSIONS

Tidal salt marsh habitats are under increasing pressure from urbanization within SF Bay, a region that contains marshes with higher primary productivity when compared to other climate regions (Kelly and Tuxen, 2009). Recent studies have found that the majority of marsh areas within SF Bay will not be able to keep pace with current SLR rates unless they sufficiently increase in elevation through accretion of sediment and organic matter (Takekawa *et al*., 2013; Thorne *et al*., 2014). Acquiring accurate elevation data is necessary to monitor the future health of these essential ecological areas. Although LIDAR provides a high density of points, higher vertical accuracy is needed in these salt marsh areas that have relatively small variations in elevation. To create accurate LIDAR-derived DEMs for tidal salt marshes, our research calls for more advanced LIDAR sensors that can deliver higher vertical accuracy by penetrating vegetation canopies and improved planning techniques that involve acquiring LIDAR, RTK GPS, and local vegetation data concurrently, as well as advanced research on DEM generation and accuracy assessment.

In this study, we examined the feasibility of using RTK GPS and vegetation data to improve the vertical accuracy of a LIDAR-derived DEM. The methods outlined in this paper were based on those applied to a salt marsh along the Atlantic coast (Hladik and Alber, 2012). We demonstrated transferability of those methods to salt marshes found along the Pacific coast and confirmed that the methods serve as a robust protocol to assess and modify LIDAR-derived salt marsh DEMs. Our research found that the Original 1-m LIDAR-derived DEM overestimated 95% of ground elevations. RMSE in the Original DEM was 0.212 m, among which the LIDAR sensor system accounted for no more than 0.0925 m and the remaining vertical error was primarily attributable to laser penetration difficulty and vegetation classification errors. Applying vegetation-specific correction factors improved the DEM's accuracy significantly, with 95% of the

vertical errors being reduced to 0.137 m or less. This Modified DEM will benefit future salt marsh research and management efforts, such as long-term SLR modeling, habitat conservation, and tidal salt marsh rehabilitation, many of which are currently underway within SF Bay and all of which rely on an accurate DEM (Brand *et al*., 2012; Goals Project, 1999; May, 2013). Research evaluating ecosystem resiliency and marsh sustainability (Schile *et al*., 2014; Stralberg *et al*., 2011; Swanson *et al*., 2013; Thorne *et al*., 2014) will also benefit from highly accurate salt marsh DEMs for use with current modeling techniques. In particular, a salt marsh DEM with reduced vertical error could offer a comparison to previous modeling efforts when used for initial marsh elevation input.

ACKNOWLEDGMENTS

Appreciation goes to Karen Thorne, Kevin Buffington, and Chase Freeman of the USGS Western Ecological Research Center for the use of their RTK GPS data. Specific gratitude is given to Lisa Schile and Kristin Byrd for their wealth of knowledge on the subject matter and guidance on study design. Funding support for MCF was provided by a grant under the Federal Coastal Zone Management Act, administered by NOAA's Office of Ocean and Coastal Resource Management and awarded to San Francisco State University.

LITERATURE CITED

Allen, J.; Cunningham, M.; Greenwood, A., and Rosenthal, L., 1992. *The Value of California Wetlands: An Analysis of Their Economic Benefits*. Oakland, California: The Campaign to Save California Wetlands, 15p.

Arkema, K.; Guannel, G.; Verutes, G.; Wood, S.; Guerry, A.; Ruckelshaus, M.; Kareiva, P.; Lacaye, M., and Silver, J., 2013. Coastal habitats shield people and property from sea-level rise and storms. *Nature Climate Change,* Letters, July 14, 1–6.

Athearn, N.; Takekawa, J.; Jaffe, B.; Hattenbach, B., and Foxgrover, A., 2010. Mapping elevations of tidal wetland restoration sites in San Francisco Bay: Comparing accuracy of aerial lidar with a singlebeam echosounder. *Journal of Coastal Research*, 26(2), 312–319.

Baye, P., 2007. *Selected Tidal Marsh Plant Species of the San Francisco Estuary: A Field Identification Guide*. Berkeley, California: San Francisco Estuary Invasive Spartina Project, 97p. http://www.spartina.org/project_documents/field_guide_tide_plants_low-res_200703.pdf.

Baye, P., 2012. Tidal marsh vegetation of China Camp, San Pablo Bay, California. *San Francisco Estuary & Watershed Science*, 10(2), 1–20.

Brand, L.; Smith, L.; Takekawa, J.; Athearn, N.; Taylor, K.; Shellenbarger, G.; Schoellhamer, D., and Spenst, R., 2012. Trajectory of early tidal marsh restoration: Elevation, sedimentation and colonization of breached salt ponds in northern San Francisco Bay. *Ecological Engineering*, 42, 19–29.

Byrd, K.; Kelly, N.M., and Dyke, E.V., 2004. Decadal changes in a pacific estuary: A multi-source remote sensing approach for historical ecology. *GIScience and Remote Sensing*, 41(4), 347–370.

Byrd, K.; O'Connell, J.; Di Tommaso, S., and Kelly, M., 2014. Evaluation of sensor types and environmental controls on mapping biomass of coastal marsh emergent vegetation. *Remote Sensing of Environment*, 149, 166–180.

California Climate Action Team, 2013. *State of California Sea-Level Rise Guidance Document*. Coastal and Ocean Working Group, March 2013, 13p. http://www.opc.ca.gov/webmaster/ftp/pdf/docs/2013_SLR_Guidance_Update_FINAL1.pdf.

California National Diversity Database, 2013. *State and Federally Listed Endangered & Threatened Animals of California*. State of California, The Natural Resources Agency, Department of Fish and Wildlife, Biogeographic Data Branch, October 2013, 14p. https://www.dfg.ca.gov/biogeodata/cnddb/pdfs/TEAnimals.pdf.

Callaway, J.; Nyman, J., and DeLaune, R., 1996. Sediment accretion in coastal wetlands: A review and a simulation model of processes. *Current Topics in Wetland Biogeochemistry*, 2, 2–23.

Chassereau, J.; Bell, J., and Torres, R., 2011. A comparison of GPS and lidar salt marsh DEMs. *Earth Surface Processes and Landforms*, 36(13), 1770–1775.

Coleman, M., 2014. International LiDAR Mapping Forum (ILMF), 2014. *NCR News*, 3(1), 1–7.

El-Sheimy, N.; Valeo, C., and Habib, A., 2005. *Digital Terrain Modeling: Acquisition, Manipulation, and Applications*. Norwood, Massachusetts: Artech House, 270p.

ESRI, 2013. *ArcGIS Version 10.1*. Environmental Systems Research Institute: Redlands, California.

Flood, M., (ed.), 2004. *Vertical Accuracy Reporting for Lidar Data, Version 1.0*. ASPRS Lidar Committee (PAD), 20p. http://www.asprs.org/a/society/committees/lidar/Downloads/Vertical_Accuracy_Reporting_for_Lidar_Data.pdf.

Gesch, D., 2009. Analysis of lidar elevation data for improved identification and delineation of lands vulnerable to sea-level rise. *In:* Brock, J.C. and Purkis, S.J. (eds.), *Coastal Applications of Airborne Lidar Remote Sensing*. Journal of Coastal Research, Special Issue No. 53, 49–58.

Goals Project, 1999. *Baylands Ecosystem Habitat Goals. A Report of Habitat Recommendations Prepared by the San Francisco Bay Area Wetlands Ecosystem Goals Project*. Oakland, California: U.S. Environmental Protection Agency, San Francisco, California/S.F. Bay Regional Water Quality Control Board, 209p.

Hauser, S., 2006. *Fire Effects Information System: Distichlis spicata*. U.S. Department of Agriculture, Forest Service, Rocky Mountain Research Station, Fire Sciences Laboratory. http://www.fs.fed.us/database/feis/.

Heinzel, J. and Koch, B., 2011. Exploring full-waveform lidar parameters for tree species classificaction. *International Journal of Applied Earth Observation and Geoinformation*, 13(1), 152–160.

Hines, E., 2011. *Final Report: Golden Gate LiDAR project*. San Francisco, California: San Francisco State University, 12p.

Hladik, C. and Alber, M., 2012. Accuracy assessment and correction of a lidar-derived salt marsh digital elevation model. *Remote Sensing of Environment*, 121, 224–235.

Hladik, C.; Schalles, J., and Alber, M., 2013. Salt marsh elevation and habitat mapping using hyperspectral lidar data. *Remote Sensing of Environment*, 139, 318–330.

Hodgson, M. and Bresnahan, P., 2004. Accuracy of airborne lidar-derived elevation: Empirical assessment and error budget. *Photogrammetric Engineering & Remote Sensing*, 70(3), 331–339.

Hu, P.; Liu, X., and Hu, H. 2009. Accuracy assessment of digital elevation models based on approximation theory. *Photogrammetric Engineering and Remote Sensing*, 75(1), 49–56.

Jakubowski, M.; Guo, Q., and Kelly, M., 2013. Tradeoffs between lidar pulse density and forest measurement accuracy. *Remote Sensing of Environment*, 130, 245–253.

Kantrud, H., 1996. *The Alkali (Scirpus maritimus L.) and Saltmarsh (S. robustus Pursh) Bulrushes: A Literature Review*. National Biological Service, Northern Prairie Science Center, U.S. Department of the Interior, *Information and Technology Report 6*. http://www.npwrc.usgs.gov/resource/plants/bulrush/index.htm.

Kelly, M. and Tuxen, L., 2009. Remote sensing support for tidal wetland vegetation research and management. *In:* Yang, X. (ed.), *Remote Sensing and Geospatial Technologies for Coastal Ecosystem Assessment and Management*. Berlin: Springer-Verlag, pp. 341–363.

Kirwan, M. and Megonigal, P., 2013. Tidal wetland stability in the face of human impacts and sea-level rise. *Nature*, 504, 53–60.

Knowles, N., 2009. *Potential Inundation Due to Rising Sea Levels in the San Francisco Bay Region (Draft)*. California Climate Change Center, U.S. Geological Survey, 31p.

Leica Geosystems, 2013. *Leica RX1200 User Manual*. 214p. http://www.surveyequipment.com/PDFs/RX1200_User_en.pdf.

Liu, X; Hu, H., and Hu, P. 2014. The "M" in digital elevation models. *Cartography and Geographical Information Science*, 42(3), 235–243.

Liu, X.; Hu, P.; Hu, H., and Sherba, J., 2012. Approximation theory applied to DEM vertical accuracy assessment. *Transactions in GIS*, 16(3), 397–410.

May, K., 2013. *Adapting to Rising Tides: Sea Level Inundation Mapping*. Berkeley, California: Bay Area Automated Mapping Association Meeting, UC Berkeley, 26 September 2013.

Montane, J. and Torres, R., 2006. Accuracy assessment of lidar saltmarsh topographic data using RTK GPS. *Photogrammetric Engineering & Remote Sensing*, 72(8), 961–967.

Morris, J.; Porter, D.; Neet, M.; Noble, P.; Schmidt, L.; Lapine, L., and Jensen, J., 2005. Integrating lidar elevation data, multi-spectral imagery and neural network modelling for marsh characterization. *International Journal of Remote Sensing*, 26(23), 5221–5234.

Murakami, H.; Nakagawa, K.; Hasegawa, H.; Shibata, T., and Iwanami, E., 1999. Change detection of buildings using airborne laser scanner. *ISPRS Journal of Photogrammetry & Remote Sensing*, 54, 148–152.

National Digital Elevation Program (NDEP), 2004. *Guidelines for Digital Elevation Data, Version 1.0*. 10 May 2004, 93p. http://www.ndep.gov/NDEP_Elevation_Guidelines_Ver1_10May2004.pdf.

National Oceanic and Atmospheric Administration (NOAA), 2010. *Technical Considerations for Use of Geospatial Data in Sea Level Change Mapping and Assessment*. Silver Spring, Maryland: U.S. Department of Commerce, NOAA NOS Technical Report, NOAA National Ocean Service, 141p. http://www.csc.noaa.gov/digitalcoast/_/pdf/SLC_Technical_Considerations_Document.pdf.

NOAA National Geodetic Survey (NGS), 1983. www.ngs.noaa.gov.

NOAA NGS, 1988. www.ngs.noaa.gov.

NOAA, Office for Coastal Management (OCM), 2012. *San Francisco Bay National Estuarine Research Reserve Habitat Map, China Camp Component*. National Estuarine Research Reserve System Compliant Map. Silver Spring, MD: NOAA, OCM. Accessed at the NERRS Central Data Management Office, http://cdmo.baruch.sc.edu/.

Nicholls, R.; Hoozemans, F., and Marchand, M., 1999. Increasing flood risk and wetland loss due to global sea-level rise: Regional and global analyses. *Global Environmental Change*, 9, S69–S87.

Nordby, J.; Cohen, A., and Beissinger, S., 2009. Effects of a habitat-altering invader on nesting sparrows: An ecological trap? *Biological Invasions*, 11(3), 565–575.

Ogilvie, J., 2014. *A Technical Overview of Alberta's Wet Areas Mapping Datasets*. Alberta Land Use Knowledge Network. https://landusekn.ca/.

Phinn, S.; Stow, D., and Zedler, J., 1996. Monitoring wetland habitat restoration in southern California using airborne multispectral video data. *Restoration Ecology*, 4(4), 412–422.

Rayburg, S.; Thomas, M., and Neave, M., 2009. A comparison of digital elevation models generated from different data sources. *Geomorphology*, 106, 261–270.

Reddy, K. and Gale, P., 1994. Wetland processes and water quality: A symposium overview. *Journal of Environmental Quality*, 23(5), 875–877.

Rosso, P.; Ustin, S., and Hastings, A., 2006. Use of lidar to study changes associated with spartina invasion in San Francisco Bay marshes. *Remote Sensing of Environment*, 100, 295–306.

Sadro, S.; Gastil-Buhl, M., and Melack, J., 2007. Characterizing patterns of plant distribution in a southern California salt marsh using remotely sensed topographic and hyperspectral data and local tidal fluctuations. *Remote Sensing of Environment*, 110, 226–239.

Schile, L.; Callaway, J.; Morris, J.; Stralberg, D.; Parker, V., and Kelly, M., 2014. Modeling tidal marsh distribution with sea-level rise: Evaluating the role of vegetation, sediment, and upland habitat in marsh resiliency. *PlosOne*, 9(2), 1–14.

Schmid, K.; Hadley, B., and Wijekoon, N., 2011. Vertical accuracy and use of topographic lidar data in coastal marshes. *Journal of Coastal Research*, 27(6A), 116–132.

Silvestri, S.; Defina, A., and Marani, M., 2005. Tidal regime, salinity, and salt marsh plant zonation. *Estuarine, Coastal and Shelf Science*, 62, 119–130.

Stralberg, D.; Brennan, M.; Callaway, J.; Wood, J.; Schile, L.; Jongsomjit, D.; Kelly, M.; Parker, T., and Crooks, S., 2011. Evaluating tidal marsh sustainability in the face of sea-level rise: A hybrid modeling approach applied to San Francisco Bay. *PlosOne,* 6(11), 1–17.

Swanson, K.; Drexter, J.; Shoellhamer, D.; Thorne, K.; Cassazza, M.; Overton, C.; Callaway, J., and Tekakawa, J., 2013. Wetland accretion rate model of ecosystem resilience (WARMER) and its applications to habitat sustainability for endangered species in the San Francisco Estuary. *Estuaries and Coasts*, 37(2), 476–492.

Takekawa, J.; Thorne, K.; Buffington, K.; Spragens, K.; Swanson, K.; Drexler, J.; Schoellhamer, D.; Overton, C., and M. Casazza, 2013. Final Report for Sea-Level Rise Response Modeling for San Francisco Bay Estuary Tidal Marshes. *U.S. Geological Survey Open File Report 2013-1081*, 161p.

Thorne, K.; Elliott-Fisk, D.; Wylie, G.; Perry, W., and Tekekawa, J., 2014. Importance of biogeomorphic and spatial properties in assessing a tidal salt marsh vulnerability to sea-level rise. *Estuaries and Coasts*, 37(4), 941–951.

U.S. Department of Agriculture (USDA) National Agriculture Imagery Program, 2009. http://datagateway.nrcs.usda.gov/.

U.S. Geological Survey (USGS). *The National Map*. http://nationalmap.gov/.

USGS, 2013. *USGS National Enhanced Elevation Dataset, Appendix C*. 32p. http://gis.tn.gov/lidar_docs/Frequently%20Asked%20Questions%5B1%5D.pdf.

Vanderzee, M., 1988. Changes in saltmarsh vegetation as an early indication of sea-level rise. *In:* Pearman, G. (ed.), *Greenhouse: Planning for Climatic Change*. Melbourne: CSIRO, pp. 147–160.

Wagner, W.; Ullrich, A.; Melzer, T.; Briese, C., and Kraus, K., 2004. From single-pulse to full-waveform airborne laser scanners: Potential and practical challenges. *International Archives of Photogrammetry and Remote Sensing*, 35(B3), 201–206.

Wang, C.; Menenti, M.; Stoll, M.: Feola, A.; Belluco, E., and Marani, M., 2009. Separation of ground and low vegetation signatures in LiDAR measurements of salt-marsh environments. *IEEE Transactions on Geoscience and Remote Sensing*, 47(7), 1–10.

Webster, T., and Dias, G., 2006. An automated GIS procedure for comparing GIS and proximal lidar elevations. *Computers & Geosciences*, 32(6), 713–726.

Wilson, J., 2012. Digital terrain modeling. *Geomorphology*, 137(1), 107–121.

Wood, J.; Liu, L.; Nur, N.; Herzog, M., and Warnock, N., 2012. Abundance, species richness, and reproductive successes of tidal marsh birds at China Camp State Park, Marin County, California. *San Francisco Estuary & Watershed Science*, 10(2), 1–15.

Zedler, J., 1991. The challenge of protecting endangered species habitat along the southern California coast. *Coastal Management*, 19(1), 35–53.

Zedler, J.; Callaway, J.; Desmond, J.; Vivian-Smith, G.; Williams, G.; Sullivan, G.; Brewster, A., and Bradshaw, B., 1999. California salt-marsh vegetation: An improved model of spatial pattern. *Ecosystems*, 2(1), 19–35.